**Noname manuscript No.**
(will be inserted by the editor)

# Propagating Longitudinal Oscillations in Coronal Loops

**I. De Moortel**

Received: date / Accepted: date

**Abstract** Outwardly propagating intensity disturbances are a common feature in large, quiescent coronal loop structures. In this paper, an overview is given of the observed properties and the theoretical modelling. As a large number of events have been observed and analysed, good statistical results on the estimated parameters have now been obtained. The theoretical modelling mainly focuses on two distinct aspects, namely the observed rapid damping of the perturbations, thought to be due to thermal conduction and the origin of the driver. Leakage of the solar surface p-modes is the main candidate to explain the observed periodicity, due to the strong correlation between loop position and period and the filamentary nature of the observed coronal intensity perturbations. Recent observational results appear to confirm the leakage and subsequent upward propagation of the solar surface 5 minute oscillations into the overlying atmospheric layers.

**Keywords** First keyword · Second keyword · More

## 1 Introduction

Using observed waves and oscillations, coronal seismology aims to deduce properties of the solar atmosphere (Uchida 1970; Roberts et al 1984). This indirect approach can provide information on physical parameters which are difficult to measure directly such as the coronal magnetic field strength (Nakariakov & Ofman 2001). During the last decade or so, a multitude of waves and oscillations have been observed in a wide variety of solar structures, turning the theoretical idea of coronal seismology into a vibrant research area (De Moortel 2005; Nakariakov & Verwichte 2005; Erdélyi 2006a; Banerjee et al 2007). From oscillations in plumes, prominences and loops to global perturbations covering a large part of the solar disk, waves seem ubiquitous in the atmosphere of our Sun. This omnipresence of waves and oscillations in the solar atmosphere was recently

I. De Moortel
School of Mathematics & Statistics, North Haugh, St Andrews, KY16 9SS, UK
Tel.: +44-1334-463757
Fax: +44-1334-463748
E-mail: ineke@mcs.st-and.ac.uk

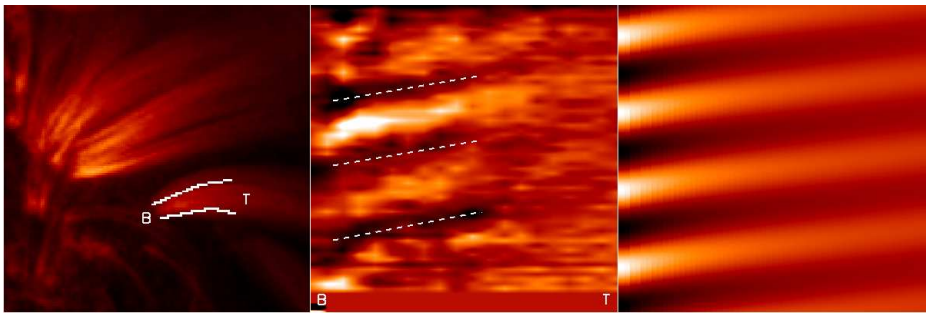


**Fig. 1** An example (TRACE 171 Å - 7 April 2000, 1242 UT) of a coronal loop footpoint (*Left*) supporting an oscillatory signal and the observed (*Middle*) and theoretically predicted (*Right*) running difference between the intensity timeseries, in which the propagating intensity disturbances are seen as bright and dark, diagonal bands.

confirmed observationally (Tomczyk et al 2007; De Pontieu et al 2007; Erdélyi & Fedun 2007; VanDoorsselaere et al 2008). Apart from coronal seismology applications, detecting oscillations in the solar atmosphere will allow us to evaluate the relative importance of wave-based heating mechanisms (Walsh & Ireland 2003; De Moortel et al 2008).

The waves described in this review paper are unique among the observed examples, in the sense that they are not excited by a nearby explosive or impulsive event but appear to be generated by an underlying driver. As such, they might be able to tell us something about the connectivity of the solar atmospheric layers. In Section 2 of this paper, the observed properties are described, paying particular attention to the periodicity and filamentary nature of the perturbations. Section 3 gives an overview of some of the theoretical modelling, focusing mainly on the damping of the coronal perturbations due to thermal conduction and on the results of recent forward modelling efforts. The discussion in Section 4 takes a look at the leakage of the 5 minute solar surface oscillations, thought to be the driver of the coronal oscillations, and some recent results on blue-shifted flows observed near the edges of active regions.

## 2 Observed Properties

Ofman et al (1997) reported the first observation (SOHO/UVCS) of propagating intensity perturbations along coronal plumes (see also Ofman et al 1999, 2000), followed by similar observations by DeForest & Gurman (1998) using SOHO/EIT. These intensity (and hence density) perturbations were found to travel along the plumes at approximately the local sound speed, leading to an early identification as propagating slow magnetoacoustic modes. Subsequently, similar propagating disturbances have been observed in coronal loops using SOHO/EIT (e.g. Berghmans & Clette 1999), TRACE (e.g. Schrijver et al 1999; Nightingale et al 1999; De Moortel et al 2000) and even Yohkoh/SXT (Berghmans et al 2001). In certain types of coronal loops, these intensity perturbations appear to be a common phenomenon and hence, they have been studied extensively, both observationally and theoretically (De Moortel 2006).

Often found in large, quiescent loops near the edges of active regions (above plage areas - see Fig. 1 left) or above sunspot umbras, the propagating disturbances show up

| | Speed (km/s) | Wavelength |
|---|---|---|
| Nightingale et al (1999) | 130–190 | 171 & 195 |
| Schrijver et al (1999) | 70–100 | 195 |
| Berghmans & Clette (1999) | 75–200 | 195 |
| De Moortel et al (2000) | 70–165 | 171 |
| Robbrecht et al (2001) | 65–150 | 171 & 195 |
| Berghmans et al (2001) | ∼300 | SXT |
| De Moortel et al (2002a) | 122 ± 43 | 171 |
| King et al (2003) | 25–40 | 171 & 195 |
| McEwan & De Moortel (2006) | 98 ± 6 | 171 |

**Table 1** Overview of the periodicities and propagation speeds of propagating slow MHD waves detected in coronal loops.

| Parameter | Average | Range |
|---|---|---|
| Oscillation Period, P | $284.0 \pm 10.4$ s | $145 - 550$ s |
| Propagation Speed, $v$ | $99.7 \pm 3.9$ km s$^{-1}$ | $O(45) - O(205)$ km s$^{-1}$ |
| Relative Amplitude, A | $3.7\% \pm 0.2\%$ | $0.7 - 14.6\%$ |
| Detection Length, $L_d$ | $8.3 \pm 0.6$ Mm | $2.9 - 23.2$ Mm |
| Energy Flux, F | $313 \pm 26$ erg cm$^{-2}$ s$^{-1}$ | $68 - 1560$ erg cm$^{-2}$ s$^{-1}$ |

**Table 2** Statistical overview of the averages and ranges of the physical properties of the 63 oscillations in coronal loop footpoints analysed by De Moortel et al (2002a) and McEwan & De Moortel (2006). Note that the uncertainty in the parameters is taken to be the standard error in the mean, $\sigma_M$. (Taken from McEwan & De Moortel 2006.)

as very small amplitude intensity perturbations. Indeed, very often, running difference images have to be used, in which the disturbances can be identified as bright and dark diagonal bands (Fig. 1 middle). A large number of examples observed by TRACE has been analysed in detail (De Moortel et al 2002a,b; McEwan & De Moortel 2006) and some of the properties summarised by McEwan & De Moortel (2006) are given in Table 2. Amplitudes are in the range of about 4% of the background intensity in the corona but higher amplitudes tend to be observed in cooler, transition region lines (see also Sect. 3.1). As mentioned above, the estimated speeds are generally of the order of the corresponding sound speeds. For the examples in McEwan & De Moortel (2006), observed in TRACE 171 Å (∼ 1 MK), propagation speeds of the order of v $\approx 99.7 \pm 3.9$ km/s are found. Table 1 shows an overview of speeds estimated by different authors, using different wavelength observations. In all cases, the estimates are likely to be a lower limit because of projection effects. Significantly, there appears to be no evidence of downward propagation, with all the observed examples so far only showing upward propagation at a largely constant speed. McEwan & De Moortel (2006) estimated that the energy flux associated with the propagating disturbances is of the order of $313 \pm 26$ ergs/cm$^2$s (compared to the $\sim 10^6$ ergs/cm$^2$s needed to keep a coronal loop at a temperature of about a million degrees). Clearly, this observed energy flux is several orders of magnitude too small to account for the heating of coronal loops but Tsiklauri & Nakariakov (2001) pointed out that a wide spectrum of slow waves could provide a significant contribution to the heating of the coronal loops.

### 2.1 Periodicity

The perturbations are generally found to be quasi-periodic, with roughly constant periods. Usually these periods are found to persist for about ∼5 cycles, although in

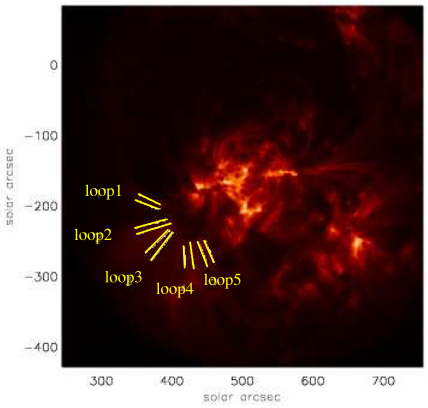


**Fig. 2** TRACE 171 Å image of AR0345 on May 3rd 2003, showing the five loop strands which support propagating intensity perturbations (adapted from McEwan & De Moortel 2006).

| Time (UT) | Oscillating Strand |
|---|---|
| 1605 | 2,5 |
| 1740 | 5 |
| 1834 | 3 |
| 1858 | 4,5 |
| 2012 | 2,5 |
| 2301 | 1 |
| 2321 | 1,2,5 |

**Table 3** Table showing that certain loop strands oscillate distinctly. For example, strand 2 is oscillating at 1605UT, not at 1740UT but again at 2012UT (taken from McEwan & De Moortel 2006).

some cases, they can last for several hours or longer (see De Moortel et al 2002a). Time-dependent methods such as wavelet analysis or periodograms are often used to determine the periods. This type of method is preferrable over, for example, Fourier analysis, due to the non-stationary nature of the observed signals. For the 63 examples analysed by McEwan & De Moortel (2006), periods ranging from 145 to 550 seconds were encountered, with an average of $284.0 \pm 10.4$ seconds. Other authors have found periods of the same order (i.e. order of minutes). However, looking in more detail at the location of the loops supporting these propagating oscillations, De Moortel et al (2002c) found that loops situated above sunspot umbras show oscillations close to three minutes, whereas non-sunspot loops (above plage regions) show oscillations closer to five minutes. It is this close link between observed periodicity and location that suggests the disturbances are driven by the (underlying) global solar surface oscillations (p-modes) (see Sect. 4.1).

## 2.2 Filamentary Nature

Very often the intensity perturbations are observed in large fan-like structures, with different loops strands oscillating at different times, but generally showing similar properties. An example of such a fan structure is shown in Fig. 2 and five individual loop

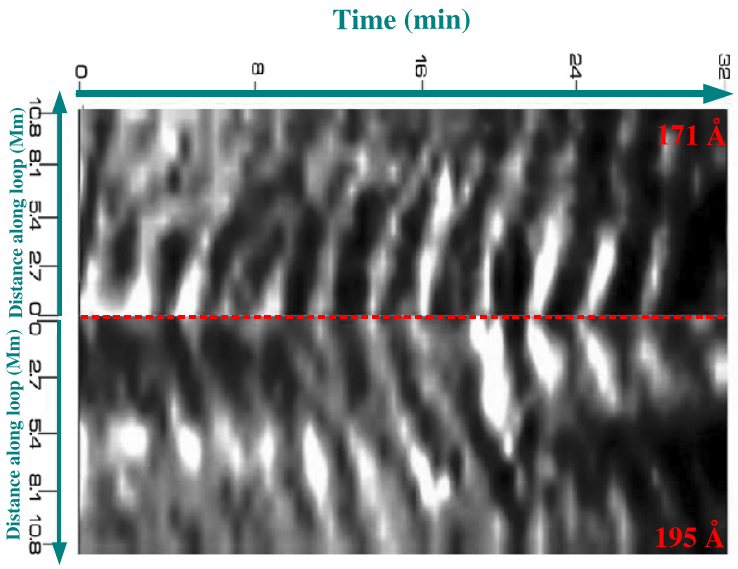


**Fig. 3** Running Difference in TRACE 171 Å (*top*) and 195 Å (*bottom*), adapted from King et al (2003).

strands which were found to support oscillations have been highlighted. Over a time interval of several hours on 3rd May 2003, propagating disturbances were found at distinct times, switching on and off quasi-periodically (see Table 3). This intermittent behaviour suggests the driver has a quasi-periodic nature, acting on spatial scales of a few Mm in diameter, i.e. the scale of the strand dimensions (McEwan & De Moortel 2006). The global solar surface oscillations exhibit a similar intermittent nature, supporting the suggestion that 5 min p-modes can leak up into some coronal loops (Baudin et al 1996; De Pontieu et al 2003b, 2004, 2005; Marsh et al 2003 - see also Sect. 4.1).

Similar evidence of this filamentary nature was presented by Robbrecht et al (2001) and King et al (2003), who compare observed propagating disturbances in different passbands. As slow waves travel at approximately the local sound speed (which strongly depends on temperature), observations of the intensity perturbations in different passbands (and hence at different temperatures) are expected to travel at different speeds (see for example Table 1). Indeed, Robbrecht et al (2001) compared observations made by SOHO/EIT (195 Å - $T \sim 1.5$ MK) with simultaneous observations by TRACE (171 Å - $T \sim 1.0$ MK) and found that the perturbations in EIT propagate slightly faster. Similarly, King et al (2003) compare the TRACE 195 Å and 171 Å passbands. The running difference studied by King et al (2003) is shown in Fig. 3. The top and bottom panels show the running difference of the 171 Å and 195 Å signals, respectively. Studying the correlation (as a function of distance along the loop) between these disturbances observed in different passbands, the authors report a progressive deterior-

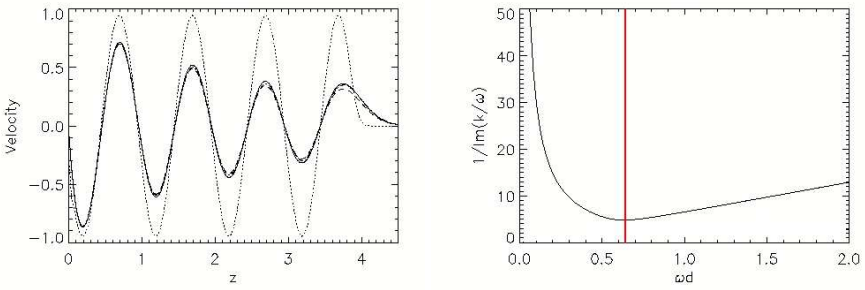


**Fig. 4** (*Left*) Perturbed velocity as a function of (dimensionless) height (dotted: ideal result; solid: thermal conduction; dot-dashed: thermal conduction + compressive viscosity; dashed: thermal conduction + optically thin radiation). (*Right*) Damping length as a function of the thermal conduction parameter $d$ (see De Moortel & Hood (2003) for the exact definition of $d$). The vertical red line indicates the minimum damping length which can be achieved with thermal conduction alone.

ation: the perturbations start off highly correlated near the base of the loop but as they propagate along the loop, the correlation gradually decreases. This loss of coherence naturally follows from the different propagation speeds associated with the different temperatures and the authors suggest it could indicated the presence of sub-resolution fine structure in the coronal loop system.

## 3 Theoretical Modelling

The combination of the observed properties indicated that the propagating disturbances are likely to be slow magneto acoustic waves and theoretical modelling confirming this interpretation was presented by Nakariakov et al (2000). The main factors influencing the evolution of the perturbation amplitudes are dissipation (causing decay) and gravitational stratification (leading to an amplitude increase). Subsequently, further geometrical effects such as the inclination angle were studied by Tsiklauri & Nakariakov (2001).

The propagation and damping of the observed slow magneto acoustic waves was studied in more detail in a series of papers by De Moortel & Hood (De Moortel & Hood 2003, 2004; De Moortel et al 2004). In this series of studies, an isothermal (coronal) plasma was considered and the combined effect of thermal conduction, compressive viscosity and optically thin radiation, as well as the effects of gravitational stratification and a diverging magnetic field geometry were investigated. In a first paper, De Moortel & Hood (2003) compared the impact of thermal conduction, compressive viscosity and optically thin radiation. All three are expected to lead to a decay of the wave amplitude as the perturbations travel along the loop. The results of this initial study are summarised in Fig. 4. The left hand side figure shows the perturbed velocity, generated on the lower boundary as a harmonic oscillation with a period of 300 seconds. As a reference value, the dotted line shows the ideal, undamped result. The solid line corresponds to the velocity perturbation damped by thermal conduction. The dot-dashed and dashed lines show the results for thermal conduction plus compressive viscosity and thermal conduction plus optically thin radiation, respectively. Comparing the three damped curves, it is immediately obvious that the main decay of the wave

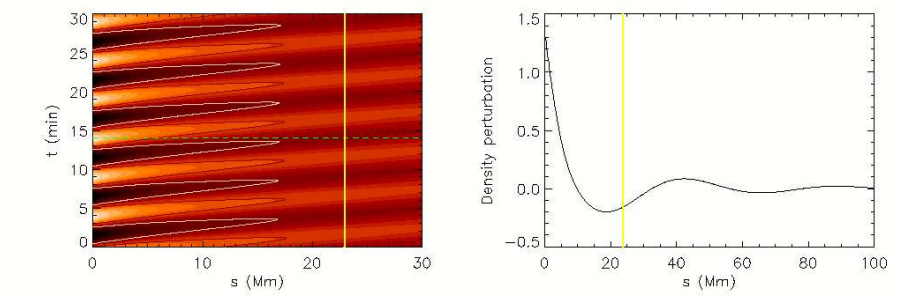


**Fig. 5** (*Left*) Contour plot of the perturbed density. The solid contours indicate where the density has decayed to about 30% of its initial value. (*Right*) A cross-section of the perturbed density at $t \approx 14$ min (green dashed line). The vertical yellow line indicates the maximum detection length of 23 Mm reported by McEwan & De Moortel (2006).

amplitude is caused by thermal conduction, and that the additional effect of either compressive viscosity or optically thin radiation is minimal. Note however that this is only true for the equilibrium conditions used in this specific numerical simulation, i.e. $T \approx 10^6$ K, $n \sim 10^9$ cm$^{-3}$. Having established the dominant effect of thermal conductivity, De Moortel & Hood (2003) continued to investigate the possibility of matching the observed very rapid damping by increasing thermal conduction. However, from Fig. 4 (right), we can see that there is actually a minimum damping length (vertical red line) that can be obtained by thermal conduction alone and increasing thermal conductivity further does no longer lead to an additional decay of the wave amplitudes. In the limit of very large conductivity, the perturbations are only weakly damped and additionally, travel at the slower, isothermal sound speed (De Moortel & Hood 2003). More recently, Owen et al (2009) demonstrated that the presence of thermal conduction causes a small phase shift between the wave velocity, energy and density. When a non-uniform equilibrium temperature is present (non-isothermal loop), this phase shift varies along the loop. Such a phase shift might be detectable when comparing oscillations in observed Doppler shifts and intensities.

Most of the loops that support propagating disturbances show a small amount of expansion near the footpoint region, i.e. where the intensity perturbations are observed. Hence, De Moortel & Hood (2004) extended the first study to include not only thermal conduction but also the effect of area divergence, as well as gravitational stratification. Both area divergence and thermal conduction are expected to cause a progressive decay of the wave amplitude whereas gravitational stratification, on the other hand, will cause the wave amplitudes to increase. Investigating these competing effects, De Moortel & Hood (2004) showed that a combination of thermal conduction and area divergence can still account for the observed damping, even when gravitational stratification is present. Fig. 5 (left) shows a (coloured) contour plot of the density perturbations, including area divergence, gravitational stratification (scale height $H \approx 50$ Mm) and thermal conduction. The solid contours show where the density perturbations have fallen off to about 30% of their initial value. Analysis of the observational data showed that this is roughly the level below which the (intensity) perturbations are no longer picked up above the 99% confidence level by the wavelet analysis. In this case, the perturbations would only have been detected (solid contours) in the first 10 - 20 Mm along the loop. The vertical (yellow) line shows the largest detection length (23 Mm)

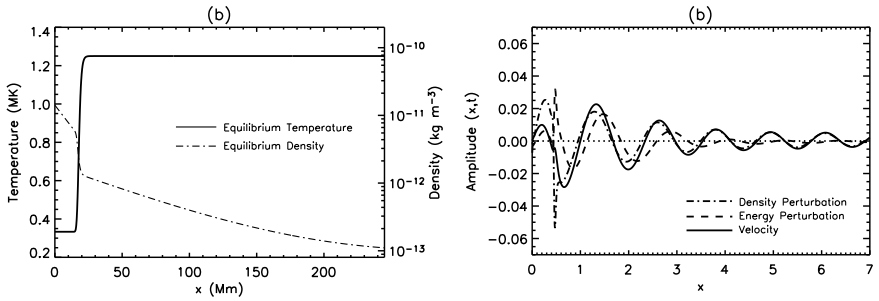


**Fig. 6** (*Left*) Model atmosphere used in the 1D simulations of Owen et al (2009). (*Right*) Perturbed velocity (solid), density (dot-dashed) and energy (dashed) as a function of (dimensionless) height generated by a harmonic driver (from Owen et al 2009).

found in the observational data (see Table 5 in McEwan & De Moortel (2006)). A small snapshot of a similar contour plot is shown in Fig. 1 (right), confirming the qualitative agreement between this simple numerical model and the running difference image of the observed perturbations (Fig. 1 - middle). Fig. 5 (right) shows a horizontal (dashed green line in contour plot) cross-section of the perturbed density, which would correspond to the pattern of the density perturbation along the loop. Again, there is a qualitative agreement with the observations; along the loop, only about one wavelength is observed before the perturbations fall below the noise level. Additional geometrical effect such as those included by Tsiklauri & Nakariakov (2001) (loop curvature, an offset of the loop centre from the base of the corona and inclination with respect to the vertical) will further decrease the effect of gravitational stratification and thus, enhance the rapid decay of the perturbation amplitudes.

Finally, De Moortel et al (2004) consider a 2D model to investigate the possible effect of a transverse density profile on the wave propagation. Such a density gradient will lead to both phase mixing and coupling between the slow and fast MHD waves. However, the efficiency of this coupling depends strongly on the value of the local plasma beta (e.g. Rosenthal et al 2002; Bogdan et al 2003), with strong coupling between the slow and fast modes only expected in regions where the sound and Alfvén speed are comparable (i.e. where $\beta \sim 1$). In the coronal environment $\beta < 1$ and De Moortel et al (2004) found indeed that the coupling between the slow and fast wave is inefficient and that this process does not extract energy from the driven slow wave fast enough to contribute significantly to the observed rapid damping. Similarly, the phase mixing of the slow waves due to the (transverse) density gradient does cause a small amount of decay of the wave amplitude but is too weak to explain the observed damping.

### *3.0.1 Non-isothermal modelling*

The models described above assumed an isothermal background, or, in other words, modelled the behaviour of the observed slow waves in the 1MK solar corona, without taking into account the propagation through the underlying atmospheric layers. The 1D model was developed further in numerical simulations by Klimchuk et al (2004), who included a non-isothermal equilibrium and non-linearity. These authors showed that unlike the density perturbations, the intensity perturbations do not depend on the

area divergence: in the non-isothermal atmosphere, the intensity variations decrease very quickly due to a combination of damping by thermal conduction and the effect of the instrument response function (TRACE 171 Å) and again, good agreement with observed values is obtained.

Similar simulations were performed by Owen et al (2009) and the model atmosphere used by these authors is shown in Fig. 6 (solid line: temperature; dot-dashed line: density). The RHS plot of Fig. 6 shows the perturbed quantities (sold line: velocity; dot-dashed line: density; dashed line: energy) in this gravitationally stratified, non-isothermal medium. The phase shift between the different perturbations mentioned above is clearly visible. Damping due to thermal conduction depends on both the temperature and density, being less efficient for lower temperatures and higher densities. Hence, for small $x$ (below the transition region), the amplitude growth due to gravitational stratification is the dominant feature. In the transition region, the efficiency of thermal conduction increases rapidly (due to the falling density and rising temperature), causing a fast decay of the perturbation amplitudes, which continues in the (isothermal) corona. Additionally, the steep transition region reflects a substantial part of the incoming wave, reducing the amplitude of the wave transmitted into the overlying corona even further.

### 3.1 Forward Modelling

Most theoretical work focusses on the behaviour of 'traditional' quantities such as velocity and density and often yields parameters that cannot easily be compared to observations. At the same time, the analysis and interpretation of observational data is subject to many possible sources of error and confusion. For the particular case of the propagating disturbances described in this paper, most of the observations so far have been done with imaging instruments, giving us intensity variations. Hence, a crucial step to ensure a direct comparison between observations and theoretical models is converting the theoretical quantities into intensities for the respective instruments. This technique is often referred to as '*forward modelling*' and allows a direct (qualitative and quantitative) comparison between observations and theory.

The fact that one cannot necessarily assume a one-to-one relation between observed (or synthesised) intensity oscillations and the associated temperature and density perturbations was recently demonstrated by e.g. Taroyan et al (2007), Taroyan & Bradshaw (2008) and De Moortel & Bradshaw (2008). Using simple analytical expressions to model (mainly) the TRACE 171 Å intensity variations resulting from decaying temperature and density perturbations, these latter authors highlighted some of the problems that can occur. Although not modelling a particular physical process, the results are directly applicable to the propagating intensity perturbations. In particular, it was found that the damping rate of the 'input' density perturbations and the resulting, synthesised intensity oscillations can be substantially different. In some cases even the periodicity can be affected and hence, great care has to be taken when interpretating observational results. In their analysis, De Moortel & Bradshaw (2008) assumed ionisation equilibrium, which will only be valid if the timescale of the perturbations is substantially larger than the ionisation and recombination rates of the relevant ions. For Fe ions in a coronal environment ($T \sim 10^6$ K - $n \sim 10^9$ cm$^{-3}$), the timescale for the Fe X and Fe XII populations to equilibrate is of the order of a few to tens of seconds, sufficiently short to warrant the assumption of ionisation equilibrium when

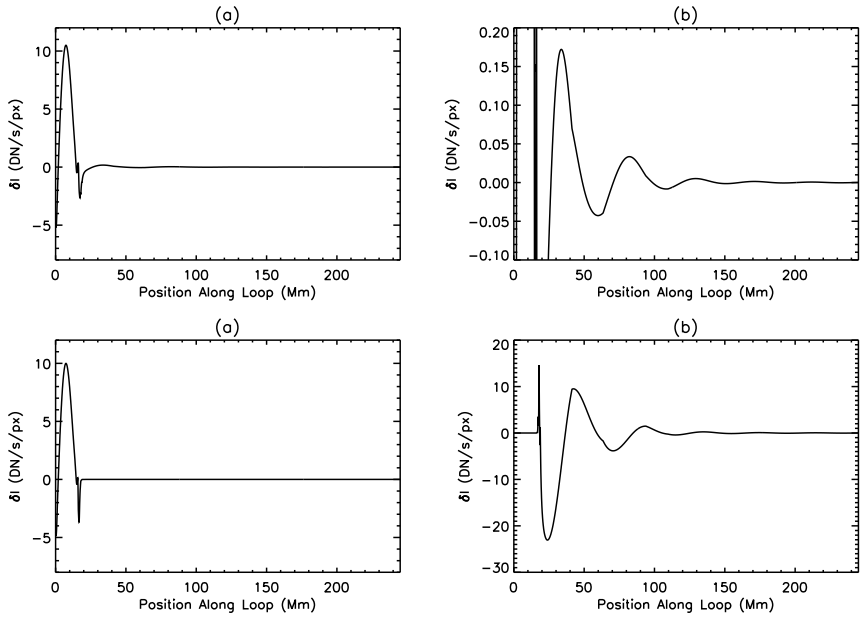


**Fig. 7** Forward modelled intensities for the perturbed quantities shown in Fig. 6: TRACE 171 Å (*Top-Left*); zoom of TRACE 171 Å focusing on the coronal part (*Top-Right*); Hinode/EIS Mg VI (*Bottom-Left*); Hinode/EIS Fe XII (*Bottom-Right*).

considering perturbations in temperature and density on timescales of a few minutes (see Table 1 in De Moortel & Bradshaw (2008)). However, for waves and oscillations at higher frequencies (say, with periods less than 1 minute), the assumption of ionisation equilibrium may no longer be appropriate, causing further complications for the interpretation of observations.

Focussing on the observed, propagating slow modes, Owen et al (2009) used the results of their numerical simulations to predict the intensity perturbations expected in TRACE and some of the SOHO/CDS and Hinode/EIS spectral lines. Fig. 7 shows the intensities (top: TRACE 171 Å ; bottom-left: EIS Mg VI; bottom-right: EIS Fe XII) resulting from the perturbations in a gravitationally stratified, non-isothermal medium (see Fig. 6 - right). As an imaging instrument, TRACE covers a relatively broad range of temperatures (compared to spectroscopic observations!) and hence, it is not surprising it picks up most of the simulated oscillations. From Fig. 7 (top-right), it is clear that the oscillations very quickly reach small amplitudes in the corona. However, Fig. 7 (top-left) shows a prominent signal in the underlying atmosphere, which is about two orders of magnitude larger than the expected coronal emission. Although there is some evidence for larger (observed) amplitudes in the transition region (e.g. O'Shea et al 2002; Brynildsen et al 2003; Marsh et al 2003), the observed difference in amplitude between transition region and coronal perturbations is much smaller. There could be several reasons for this discrepancy, not in the least the fact that the model of Owen et al (2009) is only a very simple 1D configuration. Due to their more limited temperature range, the intensities in the two chosen spectral lines only appear in more localised parts of the loop. The cooler EIS Mg VI line (Fig. 7, bottom-left) only picks up the transition region emission whereas the hotter EIS Fe XII line (Fig. 7, bottom-right)

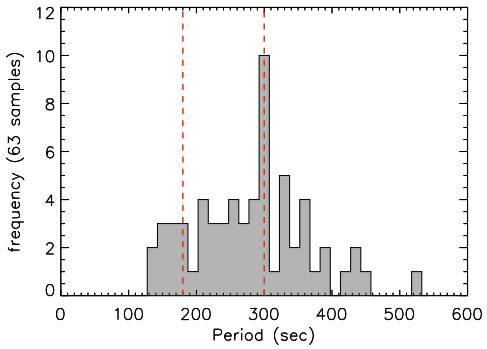


**Fig. 8** Distribution of the periodicities of the 63 propagating oscillations found from a wavelet analysis of 171 Å TRACE data (adapted from McEwan & De Moortel (2006))

.

shows the coronal part of the perturbations. Comparing the TRACE 171 Å emission (a combination of mainly Fe IX and Fe X) with EIS Fe XII (Fig. 7 right, top and bottom, respectively) shows that the 'observed' perturbations would appear almost in anti-phase. This artificial phase difference again demonstrates the need for careful interpretation of observational data, especially if one would attempt to use an observed phase difference to calculate further parameters such as the travel time.

## 4 Discussion

The periods of the observed perturbations are generally of the order of a few minutes but as mentioned in Sect. 2.1, they seem to mainly cluster around three and five minutes (see histogram in Fig. 8). De Moortel et al (2002c) showed a distinct separation in periodicty between those loops situated above sunspots ($P \sim$ three minutes) and loops above (non-sunspot) plage region ($P \sim$ five minutes). This correlation between location and period strongly suggests a link with the solar p-modes as there seems to be no other obvious reason why the observed slow modes should be characterised by such a spectrum. This implies that we are observing 'leakage' of the global solar surface modes, prompting the question: how do these modes propagate from the surface to the corona?

### 4.1 Driver

In a 'traditional model', assuming a vertical magnetic field, the five-minute p-mode is known to be trapped near the solar surface, as it is almost fully reflected in the overlying atmospheric layers. However, if one considers an inclined magnetic field, the effect of gravity along these field lines will be reduced by $\cos\theta$ (where $\theta$ is the inclination angle), allowing higher period p-modes to leak into the solar atmosphere. This was already pointed out by Bel & Leroy (1977), who demonstrated that inclining the magnetic field could provide 'magnetic portals' where five-minute p-modes can tunnel through into the overlying atmosphere. This tunneling of the traditionally 'evanescent' five minute

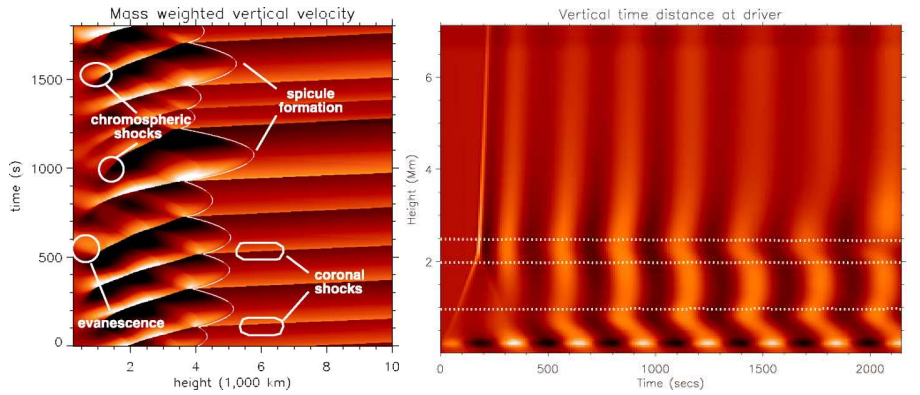


**Fig. 9** (Left) Simulated plasma velocity along an inclined ($\theta$ = 40 degrees) magnetic flux tube (De Pontieu et al 2004). (Right) Time-distance plot of the velocity at the centre of the computational domain. The horizontal dotted-lines show those regions of the domain where the cut-off frequency is exactly 300 seconds (period of the driver) (from Erdélyi et al (2007)).

p-mode has recently been the subject of a number of numerical studies. For example, De Pontieu et al (2004, 2005) and De Pontieu & Erdélyi (2006) investigate the link between the observed propagating intensity perturbations and spicules and show that p-modes with frequencies below the traditional "cut-off" frequency can indeed propagate along inclined field lines, with the degree of inclination acting as a filter to allow the propagation of certain frequencies; the photospheric oscillations leak into the overlying chromosphere where they form shocks, which in turn lead to the formation of spicules and eventually to propagation of perturbations into the corona (see Fig. 9 - left). This model was extented into 2D, including radiation and conduction by Hansteen et al (2006) and De Pontieu et al (2007), although these later papers mainly focused on the formation and behaviour of dynamic fibrils. Further studies on the leakage of the global surface oscillations into the overlying atmosphere are performed by Erdélyi and co-authors (Taroyan et al 2006; Erdélyi 2006b; Erdélyi et al 2007; Malins & Erdélyi 2007). Looking at the leakage and propagation of the surface p-modes into the overlying (non-magnetic) atmosphere (see Fig. 9 - right), these authors find that (for a 300 second driver) a range of standing modes is excited due to the interplay between a chromospheric cavity (lowest 2 dotted lines in Fig. 9 - right) and resonant excitation. Only a small fraction of the wave energy penetrates through the atmospheric layers to reach the solar corona (about 1%). The model described here is currently being extended into 3D by Fedun et al (2009).

These theoretical models of the possible leaking of the global surface oscillations have recently been complemented by observational evidence. A number of authors have observed supposedly evanescent waves and have demonstrated that their appearance is intrinsically linked to the value of the plasma $\beta$ and the inclination of the local magnetic field, which can act as magnetic portals (e.g. McIntosh & Jefferies 2006; Jefferies et al 2006; Bloomfield et al 2006; Vecchio et al 2007). For example, Vecchio et al (2007) show that the Quiet Sun can be partitioned into regions of different oscillatory connectivity, depending on the local magnetic topology (the magnetic field inclination). Perhaps even more surprisingly, Fontenla et al (1993) and Jefferies et al (2006) have analysed the energy flux contained in these low-frequency waves ($< 5$ mHz) and found that their energy flux is substantially higher than the energy flux contained in the high-frequency

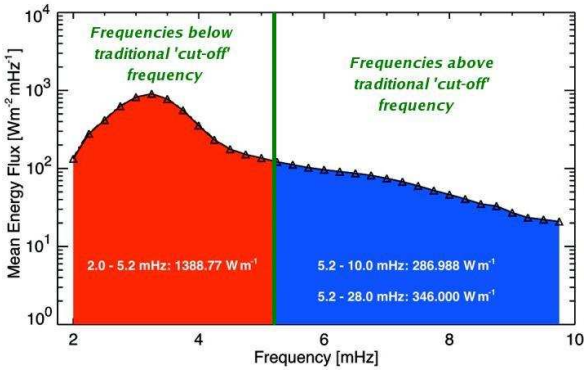


**Fig. 10** Mean energy flux found in observed chromospheric oscillations, as a function of frequency, adapted from Jefferies et al (2006).

waves ($> 5$ mHz), which had been considered (and mostly rejected) as prime candidates to account for the chromospheric heating (see Fig. 10). Hence, this result might re-open the question whether waves can account for a significant fraction of the chromospheric heating.

One can of course turn the problem around, and ask whether the observed leakage has a (significant) impact on the damping of p-modes. Turbulent damping and wave leakage are the main mechanisms proposed to account for the damping of the p-modes and a comparison with the energy flux contained in the observed coronal perturbations offers a rare opportunity to evaluate the contribution of wave leakage by direct observation. Accounting for the energy loss 'in transport', i.e. on the way between the solar surface and the lower corona is extremely difficult but De Moortel & Rosner (2007) used an order-of-magnitude calculation to show that the energy flux associated with the observed disturbances could be a significant fraction of the observed damping rate for five-minute p-modes: they estimated a coronal slow wave energy budget of the order of $10^{26}$ erg/s, compared to a p-mode damping rate of about $(2-8)\times 10^{27}$ erg/s. This simple calculation did not take into account the energy loss which is expected in the transition layers and hence is likely to be conservative. For example, De Pontieu et al (2005, 2007) and Hansteen et al (2006) suggest that the observed coronal density perturbations are remnants of chromospheric shocks, implying that only a small fraction of the *p*-mode (surface) energy will actually reach the corona. A similar conclusion was reached by Erdélyi et al (2007), who found in their (non-magnetic) numerial simulation that only 1% of the energy is actually transferred into the corona. Other processes such as e.g. mode coupling in the chromosphere and/or transition region might reduce this fraction even more.

### 4.2 Coupling of the Solar Atmosphere

The propagating intensity perturbations described in this paper offer an excellent opportunity to investigate the magnetic coupling between the underlying atmospheric layers. As the energy needed to maintain the million degree temperature of the solar corona is contained in the convective motions just below the solar photosphere, un-

derstanding how the atmospheric layers are linked and hence, how this energy can be transferred into the solar corona, is key to resolving the coronal heating question(s). A large number of waves and oscillations have now been observed in a variety of different structures, throughout the solar atmosphere (see for example other papers in this review edition or reviews by De Moortel (2005), Nakariakov & Verwichte (2005), Banerjee et al (2007)). A subset of these studies focuses on the (simultaneous) detection of oscillations in different parts of the solar atmosphere and the connectivity between them.

For example, using SOHO/SUMER observations, Wikstøl et al (2000) found small-amplitude oscillations in the transition region, driven by upwardly propagating chromospheric waves. Judge et al (2001) show that a large part of chromospheric oscillatory behaviour is dominated by the (photospheric) p-modes. However, once in the transition region, the coherence becomes less strong, which the authors suggest could be due to the interaction with the magnetic field. Several authors have highlighted the link between magnetic topology and oscillatory power or behaviour in the overlying atmospheric layers (e.g. Muglach 2003; McIntosh et al 2003, 2004; Lin et al 2005b). McAteer et al (2003) reported on propagating oscillations in chromospheric bright points, suggesting possible mode coupling between kink- and sausage-modes waves. Studying active region moss, De Pontieu et al (2003a,b) found evidence for small scale correlations between chromospheric and transition region emission in active regions.

For the three minute oscillation in sunspot umbras, several authors have demonstrated that these oscillations propagate up along the magnetic field lines, through the chromosphere and transition region, into the lower corona (e.g. O'Shea et al 2002; Brynildsen et al 2002; Rendtel et al 2003; Lin et al 2005a,b; Marsh & Walsh 2006). For the 5 minute oscillation, there is substantial (indirect) evidence, as the 5 minute oscillations have been detected in a wide variety of coronal structures. However there is much less direct observational evidence, following the propagation of the 5 minute oscillations from the surface into the corona. Baudin et al (1996) reported upwardly propagating, 5 minute, magnetoacoustic waves in the solar chromosphere and Marsh et al (2003) found evidence for $\sim$ 300 second oscillations at chromospheric (He I), transition region (O V) and coronal (Mg IX) temperatures. The observed oscillations are co-spatial and co-temporal with upwardly propagating, 5 min, oscillations observed by TRACE in a coronal loop. Similarly, O'Shea et al (2006) analyse oscillations, in an off-limb polar region, present in a range of SOHO/CDS spectral lines. The estimated phase delays between the different spectral lines indicate propagation speeds close to the local sounds speed, leading the authors to conclude that these off-limb (polar) perturbations are also likely to be outwardly propagating slow magnetoacoustic waves.

### 4.3 Outflows in Active Region Loops

Recent observations by Hinode/XRT and Hinode/EIS have found evidence for persistent, out/upward (blueshifted) flows near the edges of active regions, which some authors have linked to the slow solar wind (Sakao et al 2007; Doschek et al 2007, 2008; Del Zanna 2008; Harra et al 2008; Hara et al 2008). In almost all cases, the areas in which the outflows are observed also show enhanced line-broadening. Although at present the relation between these flows and the propagating intensity perturbations described in this paper has not been established, there do appear to be some similarities. Sakao et al (2007) report on a continuous outflow at the edge of an active region

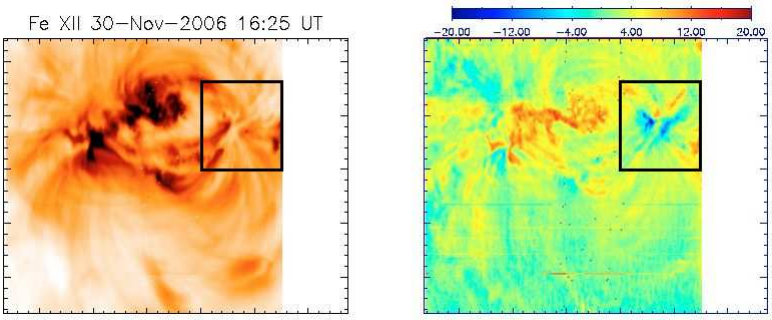


**Fig. 11** Hinode/EIS image (*Left*) and Doppler velocities (*Right*) in Active Region AR10926 (adapted from Del Zanna 2008).

(adjacent to a coronal hole) observed by Hinode/XRT (AR10942; 20-22 Feb 2007). The outflow was present for the entire 3 day observation period, with a typical velocity of the order of 140 km/s The estimated mass loss amounts to about one quarter of the mass lost rate of the solar wind. The fan like structure is situated above a collection of small sunspots, similar to some of the loops in which (3 minute) propagating intensity perturbations have been observed. Sakao et al (2007) do not mention whether there is any evidence of a periodic pattern in the observed flows. Doppler velocities measured by Hinode/EIS (Fe XII 195 Å) are of the order of 20-50 km/s, leading to outflow speeds adjusted for possible line-of-sight effects of up to 100 km/s (Harra et al 2008). Essentially the same conclusions are reached by Doschek et al (2008) for two more active regions (23 Aug and 11 Dec 2007), reporting on outflows of the order of a few km/s, up to 50 km/s, in regions of low intensity in the active regions. The temperature of the outflow region is found to be about 1.4 MK, with electron densities of the order of $5 \times 10^8$ to $10^{10}$ cm$^{-3}$. Del Zanna (2008) found both redshifts and blueshifts present in Hinode/EIS observations of AR10926 (30 Nov-3 Dec 2006). Blueshifts are mainly present in the hotter Fe lines, with speeds of the order of 5-20 km/s in FeXII and 10-30 km/s in Fe XV, again mainly in the low density regions near the edges of the active region(see rectangle highlighting fan-like loop structure in Fig. 11). Interestingly, Del Zanna (2008) also report on presence of redshifts (downflows), stronger in the cooler Fe VII line, in almost all loops within the active region, even in the fan-like loop structure at the edges. Hara et al (2008) analyse Hinode/EIS observations, following AR10938 from disk centre to the limb (18-24 Jan 2007). These authors again report similar subsonic blueshifted flows near the footpoints of the active region loops in the disk-centre observations but find that the flows decrease as the active region approaches the limb.

It is not immediately obvious how these reported outflows relate to the propagating intensity perturbations but there are some striking similarities. Both features appear to be very common in fan-like structure near the edges of active regions. The observed speeds are consistently subsonic but the blueshifts do appear to have somewhat lower speeds (of the order of tens km/s) than the propagating intensity perturbations (of the order of 100 km/s in TRACE 171 Å $\sim$ 1 MK). So far however, no periodicity in the observed outflows has been reported.

## 5 Summary

The aim of this review paper was to give an updated summary of the observations and modelling of propagating slow magnetoacoustic waves. Now observed with a variety of different instruments, these rapidly damped, small-amplitude intensity perturbations are a common feature in fan-like loop structures at the edges of coronal active regions. The observed periodicities and the filamentary nature of the propagating disturbances suggest that the global solar surface oscillations can tunnel through into the corona, providing an opportunity to study the coupling and coherence of the solar atmosphere. Both numerical modelling and observations have established that certain magnetic configurations can provide portals, allowing these p-modes to leak into the atmosphere. Forward modelling has confirmed that the observed rapid damping can be explained by thermal conduction.

Apart from the (magnetic) coupling of the atmospheric layers, the filamentary nature of the observed intensity perturbations could lead to seismology applications. At present, this is only a tentative suggestion but it certainly merits further attention. In particular, more examples are needed of co-spatial and co-temporal observations of propagating perturbations in different passbands, to establish a technique to deduce subresolution structuring from a loss of coherence between the disturbances at different temperatures. So far, the relation with blueshifts observed in similar loop structures is unclear.

**Acknowledgements** IDM acknowledges support of a Royal Society University Research Fellowship.

## References

Banerjee, D., Erdélyi, R., Oliver, R., O'Shea, E., 2007, Sol. Phys. 246,3
Baudin, F., Bocchialini, K., Koutchmy, S., 1996, A&A 314, L9
Bel, N., Leroy, B., 1977, A&A 55, 239
Berghmans, D., Clette, F., 1999, Sol. Phys. 186, 207
Berghmans, D., McKenzie, D., Clette, F., 2001, A&A 369, 291
Bloomfield, D.S., McAteer, R.T.J., Mathioudakis, M., Keenan, F.P., 2006, ApJ 652, 812
Bogdan, T.J., Carlsson, M., Hansteen, V., McMurry, A., Rosenthal, C.S., Johnson, M., Petty-Powell, S., Zita, E.J., Stein, R.F., McIntosh, S.W., Nordlund, A., 2003, ApJ 599, 626
Brynildsen, N., Maltby, P., Fredvik, T., Kjeldseth-Moe, O., 2002, Sol. Phys. 207, 259
Brynildsen, N., Maltby, P., Kjeldseth-Moe, O., Wilhelm,K., 2003, A&A 398, L15
DeForest, C.E., Gurman, J.B., 1998, ApJ 501, L217
Del Zanna, G., 2008, A&A 481, L49
De Moortel, I., Ireland, J., Walsh, R.W., 2000, A&A 355, L23
De Moortel, I., Ireland, J., Walsh, R.W., Hood, A.W., 2002*a*, Sol. Phys. 209, 61
De Moortel, I., Ireland, J., Hood, A.W., Walsh, R.W., 2002*b*, Sol. Phys. 209, 89
De Moortel, I., Ireland, J., Hood, A.W., Walsh, R.W., 2002*c*, A& A 387, L13
De Moortel, I., Hood, A.W., 2003, A&A 408, 755
De Moortel, I., Hood, A.W., 2004, A&A 415, 705
De Moortel, I., Hood, A.W., Gerrard, C.L., Brooks, S.J., 2004, A&A 425, 741
De Moortel, I., 2005, Roy. Soc. Phil. Trans. A 363, 2743
De Moortel, I., 2006, Roy. Soc. Phil. Trans. A 364, 461
De Moortel, I., Rosner, R., 2007, Sol. Phys. 246 , 53
De Moortel, I., Bradshaw, S.J., 2008, Sol. Phys. 252, 101
De Moortel, I., Browning, P.K., Bradshaw, S.J., Pinter, B., Kontar, E.P., 2008, A&G 49, Issue 3, 21
De Pontieu, B., Tarbell, T., Erdélyi, R., 2003*a*, ApJ 590, 502

De Pontieu, B., Erdélyi, R., de Wijn, A.G., 2003*b*, ApJ 595, L63
De Pontieu, B., Erdélyi, R., James, S.P., 2004, Nature 430, 536
De Pontieu, B., Erdélyi, R., De Moortel, I., 2005, ApJ 624, L61
De Pontieu, B., Erdélyi, R., 2006, Roy. Soc. Phil. Trans. A 364, 383
De Pontieu, B., Hansteen, V.H., Rouppe van der Voort, L., van Noort, M., Carlsson, M., 2007, ApJ 655, 624
De Pontieu, B. et al, 2007, Science 318, 1574
Doschek, G.A., Warren, H.P., Mariska, J.T., Muglach, K., Culhane, J.L., Hara, H., Watanabe, T., 2008, ApJ 686, 1362
Doschek, G.A., Mariska, J.T., Warren, H.P., Brown, C.M., Culhane, J.L., Hara, H., Watanabe, T., 2007, ApJ 667, L109
Erdélyi, R., 2006, Roy. Soc. Phil. Trans. A 364, 289
Erdélyi, R., 2006, ESA-SP 624, 15
Erdélyi, R., Malins, C., Tóth, G., De Pontieu, B., 2007, A & A 467, 1299
Erdélyi, R., Fedun, V., 2007, Science 318, 1572
Fedun, V., Erdélyi, R., Shelyag, S., 2009, Sol. Phys. *submitted*
Finsterle, W., Jefferies, S. M., Cacciani, A., Rapex, P., Giebink, C., Knox, A., Dimartino, V., 2004, Sol. Phys. 220, 317
Fontenla, J.M., Rabin, D., Hathaway, D.H., Moore, R.L., 1993, ApJ 405, 787
Hansteen, V.H., De Pontieu, B., Rouppe van der Voort, L., van Noort, M., Carlsson, M., 2006, ApJ 647, L73
Hara, H., Watanabe, T., Harra, L.K., Culhane, J.L., Young, P.R., Mariska, J.T., Doschek, G.A., 2008, ApJ 678, L67
Harra, L.K., Sakao, T., Mandrini, C.H., Hara, H., Imada, S., Young, P.R., Van Driel-Gesztelyi, L., Baker, D., 2008, ApJ 676, L147
Jefferies, S.M., McIntosh, S.W., Armstrong, J.D., Bogdan, T.J., Cacciani, A., Fleck, B., 2006, ApJ 648, L151
Judge, P.G., Tarbell, T.D., Wilhelm, K., 2001, ApJ 554, 424
King, D.B., Nakariakov, V.M., Deluca, E.E., Golub, L., McClements, K.G., 2003, A & A 404, L1
Klimchuk, J.A., Tanner, S.E.M., De Moortel, I., 2004, ApJ 616, 1232
Lin, C.-H., Banerjee, D., Doyle, J.G., O'Shea, E., Foley, C.R., 2005a, A & A 434, 751
Lin, C.-H., Banerjee, D., Doyle, J.G., O'Shea, E., 2005b, A & A 444, 585
Malins, C., Erdélyi, R., 2007, Sol. Phys. 246, 41
Marsh, M.S., Walsh, R.W., De Moortel, I., Ireland, J., 2003, A & A 404, L37
Marsh, M.S., Walsh, R.W., 2006, ApJ 643, 540
McAteer, R.J.T., Gallagher, P.T., Williams, D.R., Mathioudakis, M., Bloomfield, D.S., Phillips, K.J.H., Keenan, F.P., 2003, ApJ 587, 806
McEwan, M.P., De Moortel, I., 2006, A & A, 448, 763
McIntosh, S.W., Fleck,B., Judge, P.G., 2003, A&A 405, 769
McIntosh, S.W., Fleck,B., Tarbell, T.D., 2004, ApJ 609, L95
McIntosh, S.W., Jefferies, S.M., 2006, ApJ 647, L77
Muglach, K., 2003, A&A 401, 685
Nakariakov, V.M., Verwichte, E., Berghmans, D., Robbrecht, E., 2000, A&A 362, 1151
Nakariakov, V.M., Ofman, L., 2001, A&A 372, L53
Nakariakov, V. M., Verwichte, E., 2005, Living Reviews in Sol. Phys. 2, 3 (http://www.livingreviews.org/lrsp-2005-3)
Nightingale, R.W., Aschwanden, M.J., Hurlburt, N.E., 1999, Sol. Phys. 190, 249
Ofman, L., Romoli, M., Poletto, G., Noci, C., Kohl, J.L., 1997, ApJ 491, L111
Ofman, L., Nakariakov, V.M., DeForest, C.E., 1999, ApJ 514, 441
Ofman, L., Romoli, M., Poletto, G., Noci, C., Kohl, J.L., 2000, ApJ 529, 592
O'Shea, E., Muglach, K., Fleck, B., 2002, A&A 387, 642
O'Shea, E., Banerjee, D., Doyle, J.G., 2006, A&A 452, 1059
Rendtel, J., Staude, J., Curdt, W., 2003, A&A 410, 315
Owen, N.R., De Moortel, I., Hood, A.W., 2009, A & A *in press*
Robbrecht, E., Verwichte, E., Berghmans, D., Hochedez, J.F., Poedts, S., Nakariakov, V.M., 2001, A & A 370, 591
Roberts, B., Edwin, P.M., Benz A.O., 1984, ApJ 279, 857
Roberts, B., 1991, in *Advances in Solar System MHD* (Eds. E.R. Priest & A.W. Hood), CUP, Cambridge

Rosenthal, C.S., Bogdan, T.J., Carlsson, M., Dorsch, S.B.F., Hansteen, V., McIntosh, S., McMurry, A., Nordlund, A., Stein, R.F., 2002, ApJ 564, 508
Sakao,T. et al, 2007, Science 318, 1585
Schrijver, C.J. et al., 1999, Sol. Phys. 187, 261
Taroyan, Y., Erdélyi, R., Malins, C., 2006, ESA-SP 624, 135
Taroyan, Y., Erdélyi, R., Wang, T.J., Bradshaw, S.J., 2007, ApJ 659, L173
Taroyan, Y., Bradshaw, S.J., 2008, A&A 481, L247
Tomczyk, S. et al, 2007, Science 317, 1192
Tsiklauri, D., Nakariakov, V.M., 2001, A&A 379, 1106
Uchida, Y., 1970, Pub. Astron. Soc. Japan 22, 341
Van Doorsselaere, T., Nakariakov, V.M., Verwichte, E., 2008, ApJ 676, L73
Vecchio, A., Cauzzi, G., Reardon, K.P., Janssen, K., Rimmele, T., 2007, A& A 461, L1
Walsh, R.W., Ireland, J., 2003, Astron. & Astroph. Rev 12, 1
Wikstøl, Ø., Hansteen, V.H., Carlsson, M., Judge, P.G., 2000, ApJ 531, 1150